ON THE CAUSES OF BASIS WEIGHT VARIABILITY

Project F004

Report 2

to the

MEMBER COMPANIES OF THE INSTITUTE OF PAPER SCIENCE AND TECHNOLOGY

September 1998

INSTITUTE OF PAPER SCIENCE AND TECHNOLOGY

Atlanta, Georgia

ON THE CAUSES OF BASIS WEIGHT VARIABILITY

Project F004

Report 2

A Progress Report

to the

MEMBER COMPANIES OF THE INSTITUTE OF PAPER SCIENCE AND TECHNOLOGY

By

Wang, X., Anderson, T., Snyder, C., and Marziale, M.

September 1998

On the Causes of Basis Weight Variability

by

X. Wang [†], T. Anderson [‡], C. Snyder [‡], and M. Marziale [‡]

Abstract

In this paper, we study the effects of flow rate, fiber consistency, and pressure fluctuation on basis weight variations. The set of mill operation data includes thick stock flow rate, consistency at eight different stock preparation stages, inlet and outlet pressure of the pressure pulsation attenuator, scanner position, β gauge, and scanner basis weight measurements. In order to focus on the important spectra, correlations, phase-space, and scatter diagrams of variations in the low frequency range, we employ the boxcar averaging procedure to eliminate high frequency extraneous information. We also discuss the transfer function between the input and output spectra of certain components or processes within approach flow systems. Particular emphasis is laid on the synchronization procedure necessary for the study of low frequency range signals. A specific software developed at IPST is used to automatically perform the signal analyses discussed in this paper.

[†] Institute of Paper Science and Technology, 500 10th St., N.W., Atlanta, GA 30318

[‡] Westvaco Corporation, 1724 Westvaco Rd., P.O. Box 278, Wickliffe, KY 42087

1 Introduction

Regardless of the damping features of individual headbox designs, it is important to minimize stock consistency variation and pressure fluctuation to achieve uniform and smooth stock delivery to the headbox. Various studies have been reported on the causes of basis weight variability, the most fundamental paper property. General methodology and analysis of basis weight variations have been documented in Refs. [5] [13] [6] [7] [8]. In Ref. [10], Norman and Wahren discussed in detail the mass distribution and turbulence spectra based on micro- and macro-scale descriptions. A focused investigation of wet-end vibration and its effects on basis weight was reported by Perrault [12]. In this paper, we employ a software, PMSAP (*PaperMaking Signal Analysis Package*), developed at IPST to systematically study a set of mill operation data, and provide an overview of various causes of basis weight variability. Along with the frequency analysis and correlation tools [11], we also explore the use of phase-space and scatter diagrams. To overcome the drawbacks of on-line signal processes discussed by Brendemuehl and Borchert [1], we recorded more than two hours of multichannel mill operation data with a sampling period of 0.01 sec. This enables us to focus more on the low frequency variation and perform multichannel cross correlations. Because a stable system may also have cyclic variations, which can be reflected in the final product, such comprehensive signal analyses will help to discern the key influence factors from the culmination of a long series of stock preparation process steps, and to weed out chronic system upsets.

The process variations, such as the retention level and fines, significantly affect the drainage and consequently, the system stability and are discussed in depth in Ref. [9]. In this paper, we will address the following issues: (i) consistency variations within different stages of stock preparation and their influence on the

2

basis weight; (ii) pressure pulsation effects on cross-machine direction (CD) and machine direction (MD) basis weight variations; (iii) effectiveness of the current pressure pulsation attenuator; (iv) effects of the stock flow rate on the basis weight; and (v) the correlations of stock flow rate, consistency, and pressure variations.

In the following section, we summarize the signal analysis techniques used in this work. We discuss in Section 3 the set of mill operation data and the analysis results. In the concluding section, we reiterate the key findings from the analysis of this particular set of mill data and shed new light on the practical implications of such analyses.

2   Research Approaches

We use in this work discrete signal analysis tools. Suppose we have a discrete sampling $x[n]$ of a time varying signal with a sample period T, for a time duration of interest Δt, the total number of sampling points is $N = \Delta t / T$. Moreover, we can only obtain spectrum of frequencies up to the Nyquist critical frequency $f_c = 2/T$, and the lowest sensible frequency is of course $1/\Delta t$. Denoting the frequency domain signal as $X[n]$, we have the following discrete Fourier transform:

$$x[n] \;=\; \sum_{m=0}^{N-1} X[m] e^{j2\pi nm/N} \tag{1}$$

$$X[m] \;=\; \frac{1}{N} \sum_{n=0}^{N-1} x[n] e^{-j2\pi nm/N} \tag{2}$$

Notice that with N input data points, based on the periodicity in the frequency domain, we obtain the following frequency range,

$$f_n = \frac{n}{NT}, \quad -\frac{N}{2} \leq n \leq \frac{N}{2} \tag{3}$$

3

Since Eqs. (1) and (2) are implemented as the Fast Fourier Transform (FFT) in our software PMSAP, the number of data points we select, out of more than one million data points gathered per channel, must be a power of two.

Assume that we have two functions $x(t)$ and $y(t)$, and their corresponding Fourier transforms $X(f)$ and $Y(f)$, the spectrum of their cross correlation $corr(x,y)$ can be denoted as XY^* (refer to Ref. [15]), where $*$ represents the complex conjugate. Therefore, we can easily obtain the cross correlation as well as the transfer function $H(f) = Y(f)/X(f)$ by using FFT.

The main feature of this work is to derive useful information within different frequency ranges based on signal-to-noise enhancement. The basic concept of this technique is to update a point with the average of a certain number of points around it. Of course, we assume that the signal of interest varies only slowly with time and the average of a small number of adjacent points is a better measure of the signal than any of the individual points. For example, to focus on the low frequency range up to $1/(2TN_a)$ Hz, we select one data point out of every N_a data, and the boxcar average process is illustrated as follows:

$$\hat{x}[n] = \sum_{i=(n-1)N_a+1}^{nN_a} x[i]/N_a, \quad 1 \leq n \leq \Delta t/TN_a \qquad (4)$$

where $\hat{x}$ represents the smoothed signal.

3 Data Analysis

Measurements are made of flow rate, consistency, and pressure to determine the effects on basis weight variations. We assume that the measured consistency represents the actual consistency. The measuring point locations are depicted in Fig. 1. We record all fourteen channels simultaneously for two separate runs; one has a

4

duration of more than two hours without stuff box flow rate control, and the other includes a little less than an hour long data with the flow rate control. In the ensuing signal analyses, we will synchronize the signal channels by taking into consideration the predetermined stock transit time between the measurement points, i.e., the time delays. To convert voltage measurements to physical quantities, we introduce the following calibration factors a and b:

$$y = ax + b \tag{5}$$

with

$$
\begin{aligned}
a &= (y_{max} - y_{min})/(x_{max} - x_{min}) \\
b &= (y_{min}x_{max} - y_{max}x_{min})/(x_{max} - x_{min})
\end{aligned}
$$

where y and x stand for the physical quantity and the corresponding voltage measurement, while the subscripts max and min represent the upper and lower bounds.

3.1 Overview of Signals

In Table 1, we list fourteen channels of various process variables, their corresponding calibration factors, and time delays. All fourteen channels of measured signals are presented in Figs. 2, 3, 4, and 5, which show that most of the time delays happen within the stock preparation processes, and significant time lag (nearly 52 min.) exists from various stock preparation stages to the measurement of basis weight downstream at the reel.

In general, there are a few frequency ranges of interest to paper manufacturers:

	Period (s)	Frequency (Hz)	Paper Length (m)
long term	> 200	< 0.005	$> 40,000$
medium term	$1 \sim 200$	$0.005 \sim 1$	$20 \sim 40,000$
short term	$0.1 \sim 1$	$1 \sim 10$	$2 \sim 20$
formation	< 0.1	> 10	< 2

where the machine speed (reel speed) V is assumed to be 3600 ft/min.

In this work, for simplicity, we show in all spectra the percentage fluctuation of the signal around its average. Figures 6 and 7 present a few key measurements' spectra for three frequency ranges ($\sim$ 0.25 Hz, $\sim$ 1 Hz, and $\sim$ 50 Hz). It is observed that two runs exhibit the same spectra signatures, which indicates that the spectra represent, in general, the overall stock approach flow system performance. According to the nature of the frequencies at 0.6 Hz and 30 Hz, we suspect that they are the system noise within our data acquisition process. We identify that when the control valve is active, a larger portion of the long-term variations of flow rates and pressure is random, compared with the case in which the control valve is inactive. However, the improvement of MD basis weight variation is not significant. In fact, a couple of strong variations emerge below the frequency of 0.1 Hz with the control loop activated.

In addition, a number of observations are obtained:

- The frequencies of 0.1 and 0.75 Hz show up in the thick stock flow rate variation as well as the pressure fluctuation. This can be explained by the relation $\rho \dfrac{\partial v}{\partial t} \sim \dfrac{\partial p}{\partial s}$, derived from the Navier-Stokes equation by neglecting the viscous and convection effects, where v, ρ, s, and p stand for the axial velocity component, fluid density, axial coordinate, and pressure, respectively. Surprisingly, the same frequency component shows up in the stuff box consistency measurement as well, which indicates that the consistency sensor was picking up flow variations.

- The frequency 0.75 Hz strongly affects the β gauge basis weight variation.

- The frequency 40 Hz shows up distinguishably in the scanner basis weight

6

variation, and the same frequency component exists in the pressure pulsation.

As depicted in Fig. 8, the cross correlations between the β gauge basis weight variation and various stock preparation processes within the low frequency range indicate that there is a common variation at the period of 700 s. This extremely low frequency variability, which is different from the relative high frequency "barring" discussed in Refs. [5] [4] [14], can be traced all the way back to the machine chest and high density tanks.

3.2 Pressure Pulsation

As shown in Fig. 9, the effectiveness of the pressure pulsation attenuator is quite different in three frequency ranges ($\sim$ 0.25 Hz, $\sim$ 1 Hz, and $\sim$ 50 Hz). We define the transfer function $H(f)$ as,

$$H(f) = 20log_{10}|P_{out}/P_{in}| \qquad \text{dB} \qquad (6)$$

and to better illustrate the pressure pulsation attenuator performance, we also use the boxcar average. As shown in Figs. 10, 11, and 12, the overall attenuation for the frequency higher than 1 Hz is strong, except for a strange spike around 22 Hz, which could be introduced within the headbox manifold and the recirculation line. However, the attenuator performs poorly for the frequencies below 1 Hz. Detailed discussions and a preliminary study on the current pressure pulsation attenuation device are reported in Ref. [16]. Furthermore, Figures 11 and 12 demonstrate that the time delay does not have as strong an effect on the signal analyses of the high frequency range as it does on the low frequency range. In addition, data collected during both runs share the same transfer function pattern in Figs. 11 and 12, which indicates that the transfer functions presented here are generic.

Ch #	Name	Unit	x_{min}	x_{max}	y_{min}	y_{max}	Atten.	a	b	Delay (s)
	Deck # 1									
1	Pressure (Attenuator Inlet)	(psi)	0	10	0	80	10	8	0	3105
2	Pressure (Attenuator Outlet)	(psi)	0	10	0	32	5	3.2	0	3105
3	Flow Rate (Thick Stock)	(gpm)	1	5	0	4500	10	1125	-1125	3015
4	Consistency (Stuff Box)	(%)	1	5	2	4	5	0.5	1.5	3015
5	Consistency (Duo #2 Upper)	(%)	1	5	0	20	5	5	-5	3105
6	Consistency (Duo #1 Lower)	(%)	1	5	0	5	5	1.25	-1.25	3105
7	Ground (Off)	(V)	0	1	0	1	5	1	0	0
8	Ground (On)	(V)	0	1	0	1	5	1	0	0
	Deck # 2									
1	Position (Scanner)	(ft)	1	5	0	30	10	7.5	-7.5	3115
2	Basis Weight (Scanner)	(lb/3000 ft^2)	1	5	0	80	10	20	-20	3115
3	Basis Weight (β Gauge)	(lb/3000 ft^2)	5	3.6	45	125	10	-57.14	330.71	3115
4	Consistency (Machine Chest)	(%)	1	5	2	4	5	0.5	1.5	2565
5	Consistency (Softwood)	(%)	1	5	2	5	5	0.75	1.25	0
6	Consistency (Hardwood)	(%)	1	5	2	5	5	0.75	1.25	0
7	Consistency (Blend Chest)	(%)	1	5	2	5	5	0.75	1.25	2115
8	Consistency (Blender)	(%)	1	5	2	5	10	0.75	1.25	915

Table 1: Data acquisition channel arrangements.
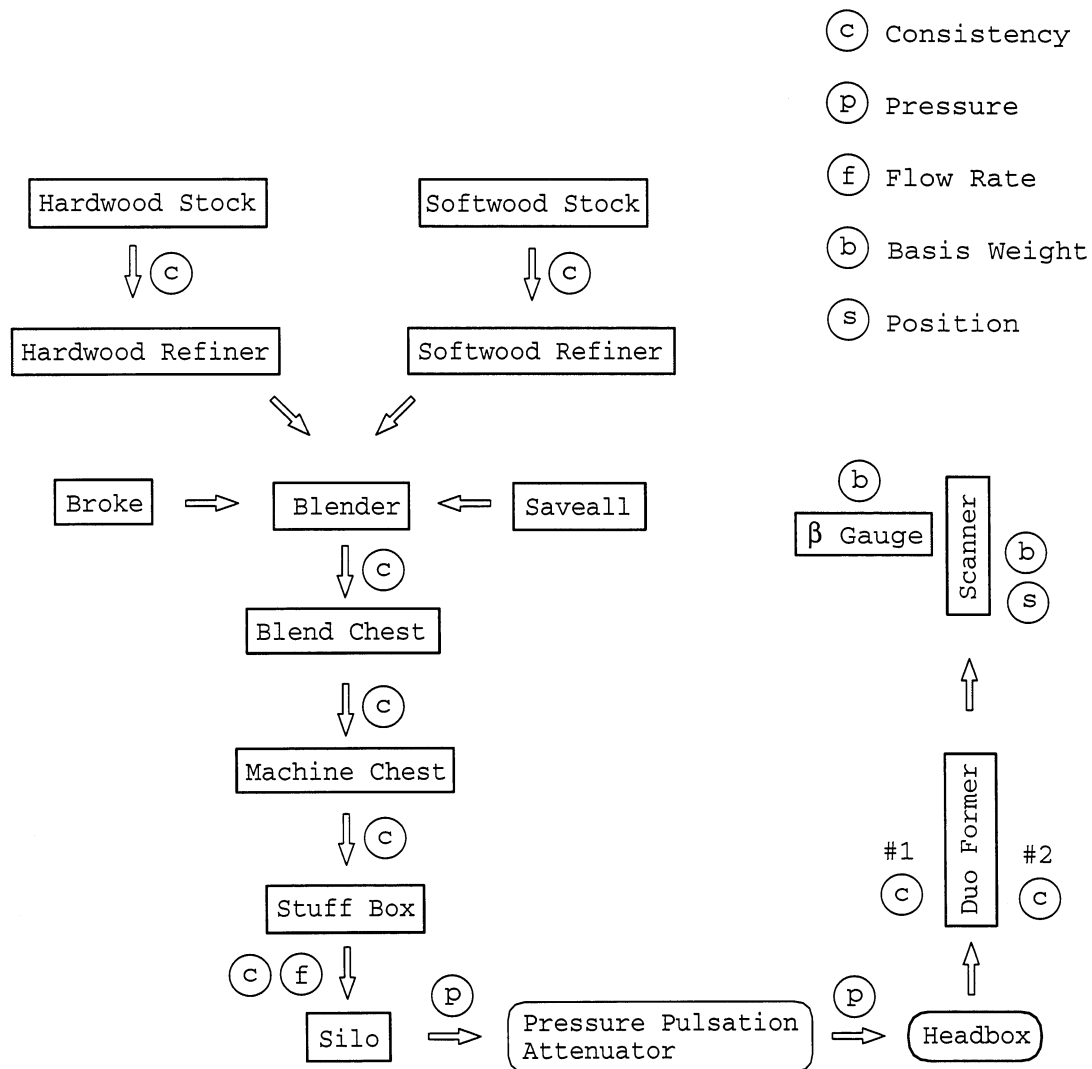
Figure 1: Measurement locations of various process variables.

3.3 Basis Weight

Basis weight (or grammage) is the commercial term used to represent the paper mass per unit area, and a common unit is lb/3000 ft^2. In general, we represent the paper basis weight variability by the sum of three components, i.e., CD variation (σ_c), MD variation (σ_m), and residual variation (σ_r) [2] [3], where the scanner basis weight variation (σ_s) satisfies

$$\sigma_s^2 = \sigma_c^2 + \sigma_m^2 + \sigma_r^2 \qquad (7)$$

In addition to the on-line scanner basis weight measurement, we also use in this work a fix point β gauge measurement. For the scanning period T_o, we have N_o sampling points per scanning period with $N_o = T_o/T$. If we select N_c CD points in cross-machine direction ($N_c < N_o/2$), we can construct the following N_c series of MD variations

$$\tilde{x}_i[n] = x_i[(n-1)N_o + i], \quad 1 \leq i \leq N_c \qquad (8)$$

where $\tilde{x}_i$ stands for the ith fix point basis weight measurement with the sampling period T_o. Furthermore, we derived the following CD profile by averaging each MD variation series $\tilde{x}_i$

$$x_c[i] = \sum_{n=1}^{N_s} \tilde{x}_i[n]/N_s \qquad (9)$$

where N_s stands for the total points within each MD basis weight measurement series $\tilde{x}_i$.

Paper basis weight is influenced by every stage of the stock preparation and paper making processes. In general, there are two types of consistency effects on

10

basis weight variations. The temporal variation of consistency can be viewed as the variation of the total fiber mass passing through a fixed pipe cross-sectional area, and it affects mainly the MD and residual basis weight variability. The spatial variation of consistency corresponds to the fiber distribution at the pipe cross section, which is often called fiber stratification. If such fiber stratifications exist before the stock enters the headbox manifold, it exerts strong effects on the CD and residual basis weight variation. A detailed study of the use of perforated plates or the reservation of enough pipe length between the last elbow turn and the headbox manifold requires the solution of three-dimensional turbulent pipe flow fields as well as the associated mass transfer equations [17].

Figure 13 shows the spectra of CD, stock flow rate, pressure, and consistency of the first run measurements. Other than the unexpected frequency at 0.6 Hz, we find in the CD basis weight spectrum,

- the frequency spikes at 1.6 Hz, 4.3 Hz, and 4.45 Hz corresponding directly to the same spikes in the pressure pulsation spectrum;

- the frequency spike at 1.8 Hz corresponding directly to the same spike in both the pressure pulsation and thick stock flow rate spectra;

- the frequency spike at 3.3 Hz corresponding directly to the same spike in the the stuff box consistency variation spectrum; and

- the frequency spike at 3 Hz existing in both the pressure pulsation and thick stock flow rate spectra disappeared.

As also shown in Fig. 14, during the second run, the stock flow control did smooth out some thick stock flow rate variation, such as the frequency spike at

11

3 Hz; however, the main features of the stuff box consistency and pressure pulsation remain the same. It is interesting to note that with the stock flow control loop, the CD profile is improved significantly.

3.4 Synchronization

As depicted in Fig. 15, both the phase-space diagram and the spectrum plot cannot represent the very low frequency correlation with the period of 700 Hz as clearly as the cross correlation curve. To better illustrate the system performance, we also use the scatter diagram to discern the stability of the process. In general, as discussed in Ref. [9], a smaller scatter area implies better stability. It is clearly demonstrated in Figs. 15 and 16 that both runs are stable.

To study the synchronization effects, we display the low frequency range cross-correlation curve between the β gauge basis weight and the machine chest consistency with and without the synchronization. As shown in Fig. 17, correlation results depend on the synchronization. Similar conclusions can be drawn from Fig. 18 as well. However, Figure 19 shows that the synchronization does not alter the scatter diagram significantly.

4 Conclusions

We have studied the large amount of information gathered in two separate runs on the same paper machine. The benefit of analyzing two sets of mill data is to confirm that some of the findings are generic and system dependent, such as the pressure pulsation attenuator performance, scatter diagram, and spectra. The most significant aspect of this work is to present a systematic approach to tackle the mill data and extract from a wealth of information packed in the signals the

most important aspects of the improvement of both system performance and future system designs.

In conclusion, we have made the following observations:

(1) Synchronization (taking into consideration the time lags) is important to analyze the low frequency range signals, and will affect corresponding correlation, transfer function, and scatter diagrams; nevertheless, synchronization is not needed for the analysis of high frequency range signals;

(2) For a particular paper machine, there exists a long-term variation with the period of ~ 700 s in the early stock preparation processes;

(3) The pressure pulsation attenuation device is effective for frequencies higher than 1 Hz, and the transfer functions obtained from the inlet and outlet pressure pulsations are characteristics of the particular pressure pulsation attenuator and the headbox recirculation line;

(4) Regardless of certain high, medium, and low frequency range variations, both runs were stable;

(5) Medium range frequency signals in the pressure pulsation, stock flow, and consistency can be introduced to the CD basis weight variation; and

(6) The use of a stuff box stock flow control valve does not improve the MD basis weight variation as significantly as the CD basis weight variation; nevertheless, we anticipate the positive effects on the system stability.

The analysis procedures and the software (PMSAP) developed at IPST can be used to study the long-term , multichannel signals of other process variables such as retention aids and fines.

5 Acknowledgment

We would like to thank the member companies of the Institute of Paper Science and Technology and specifically, Westvaco Corporation for their support.
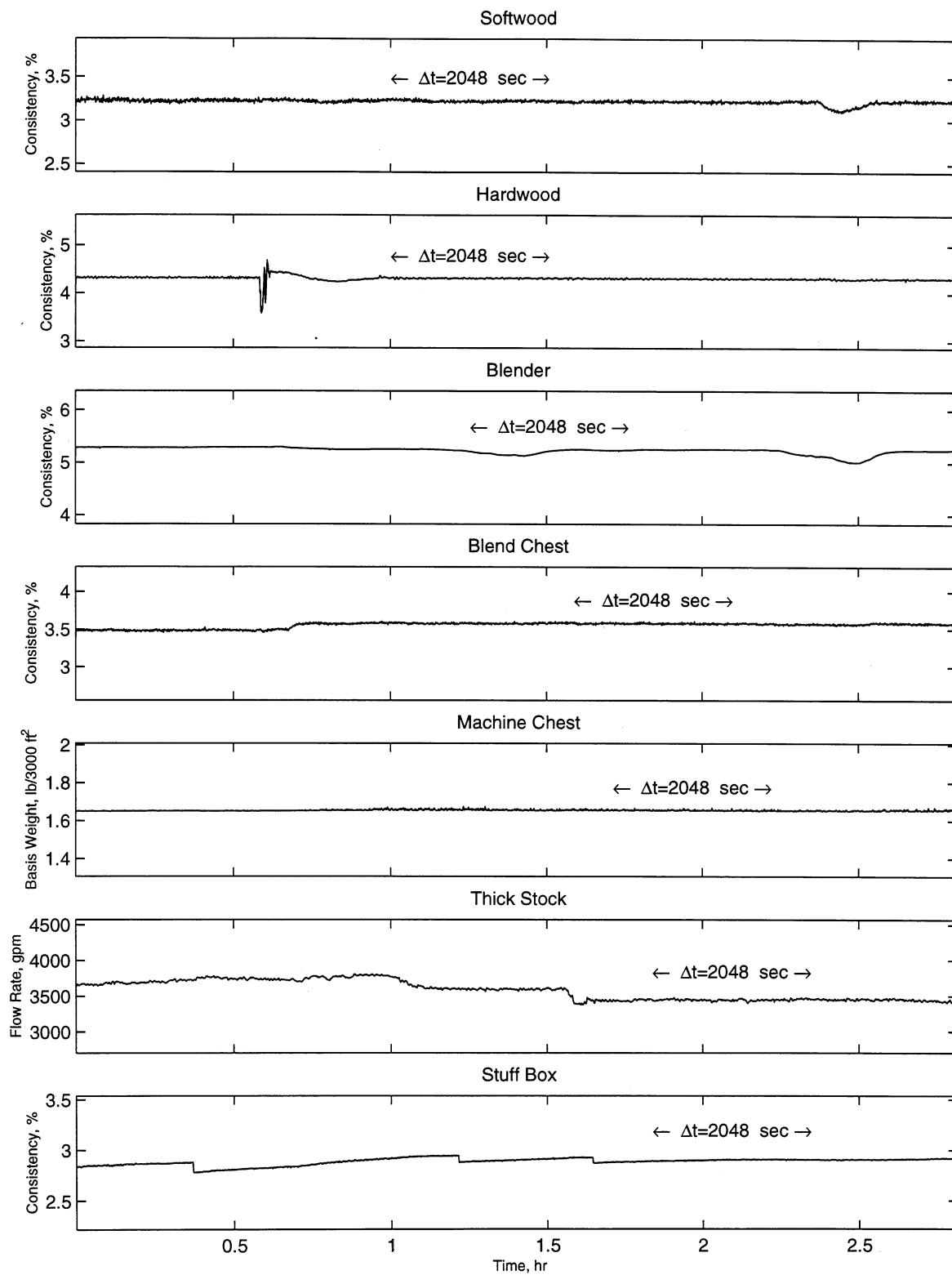
Figure 2: Changes of process variables over time # 1. (First run of 2.817 hours)

15
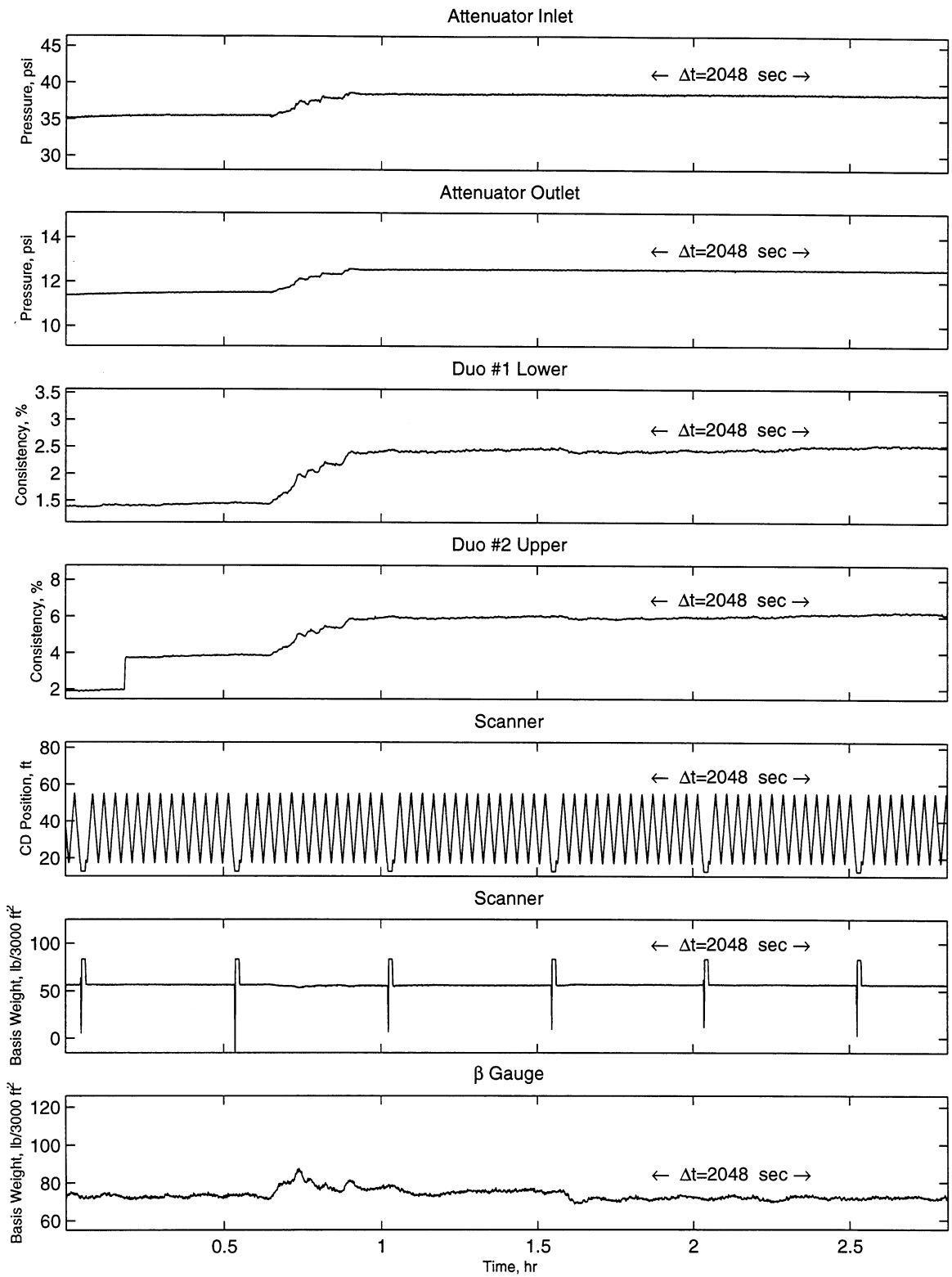
Figure 3: Changes of process variables over time # 2. (First run of 2.817 hours)
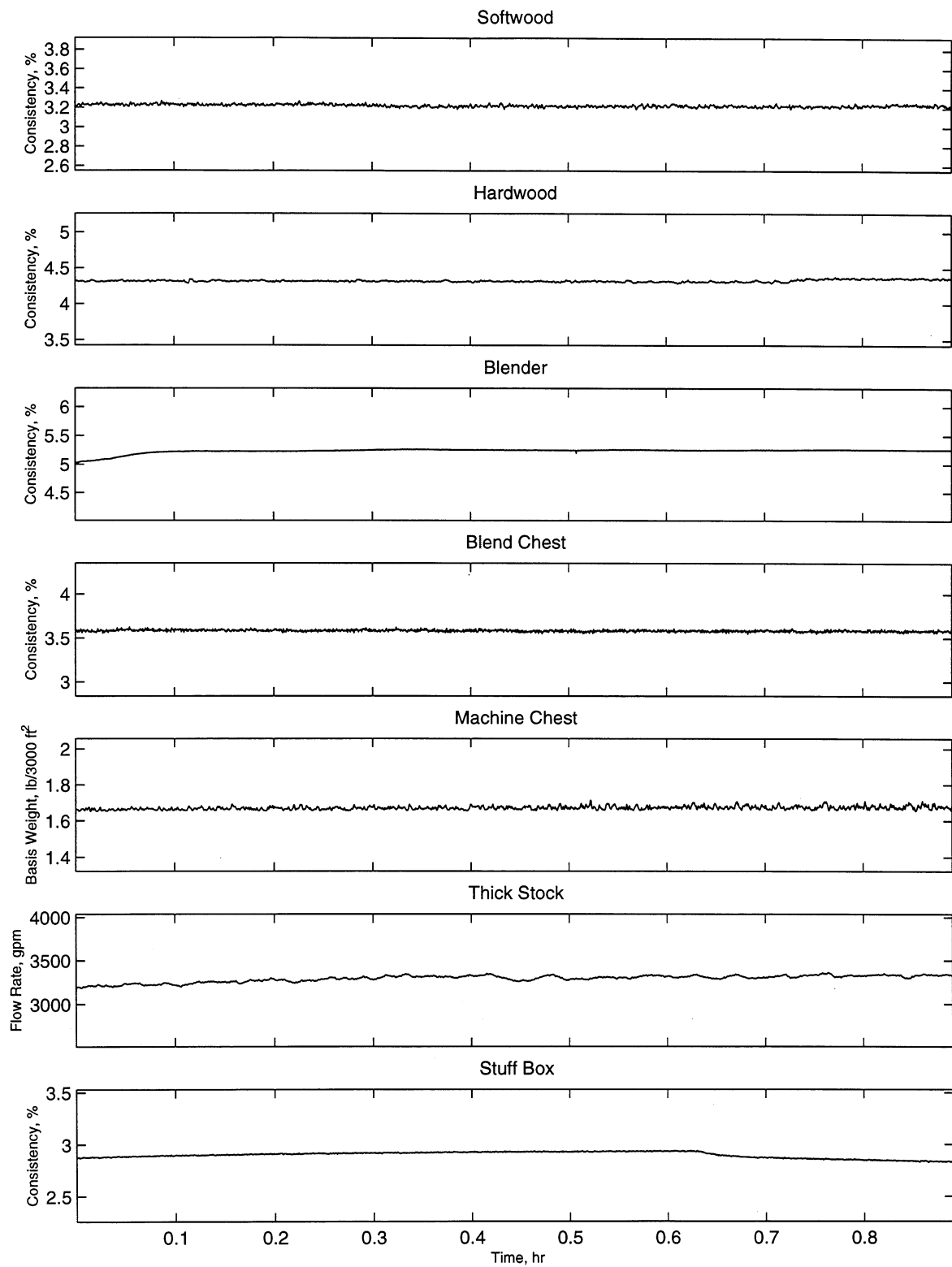
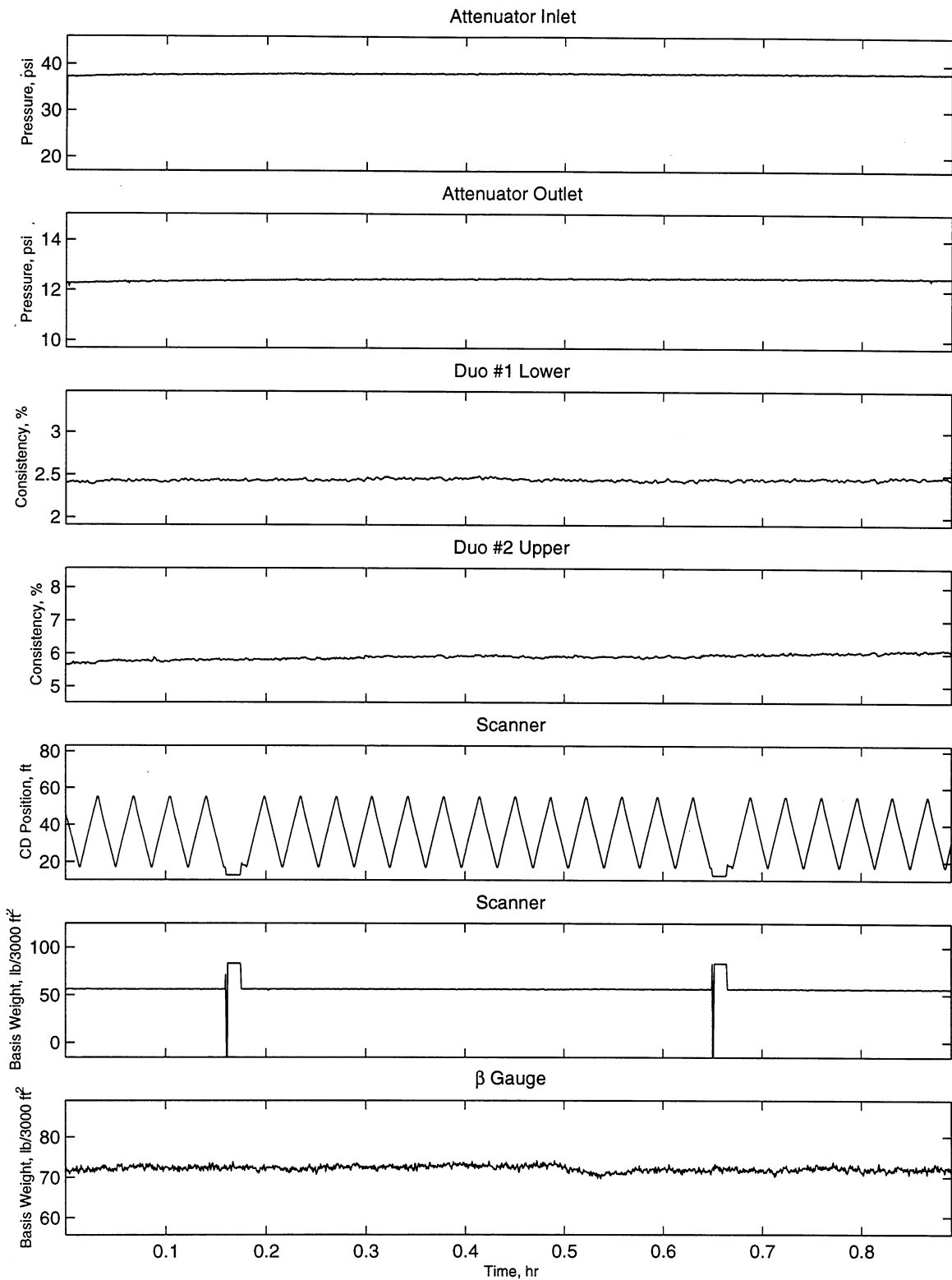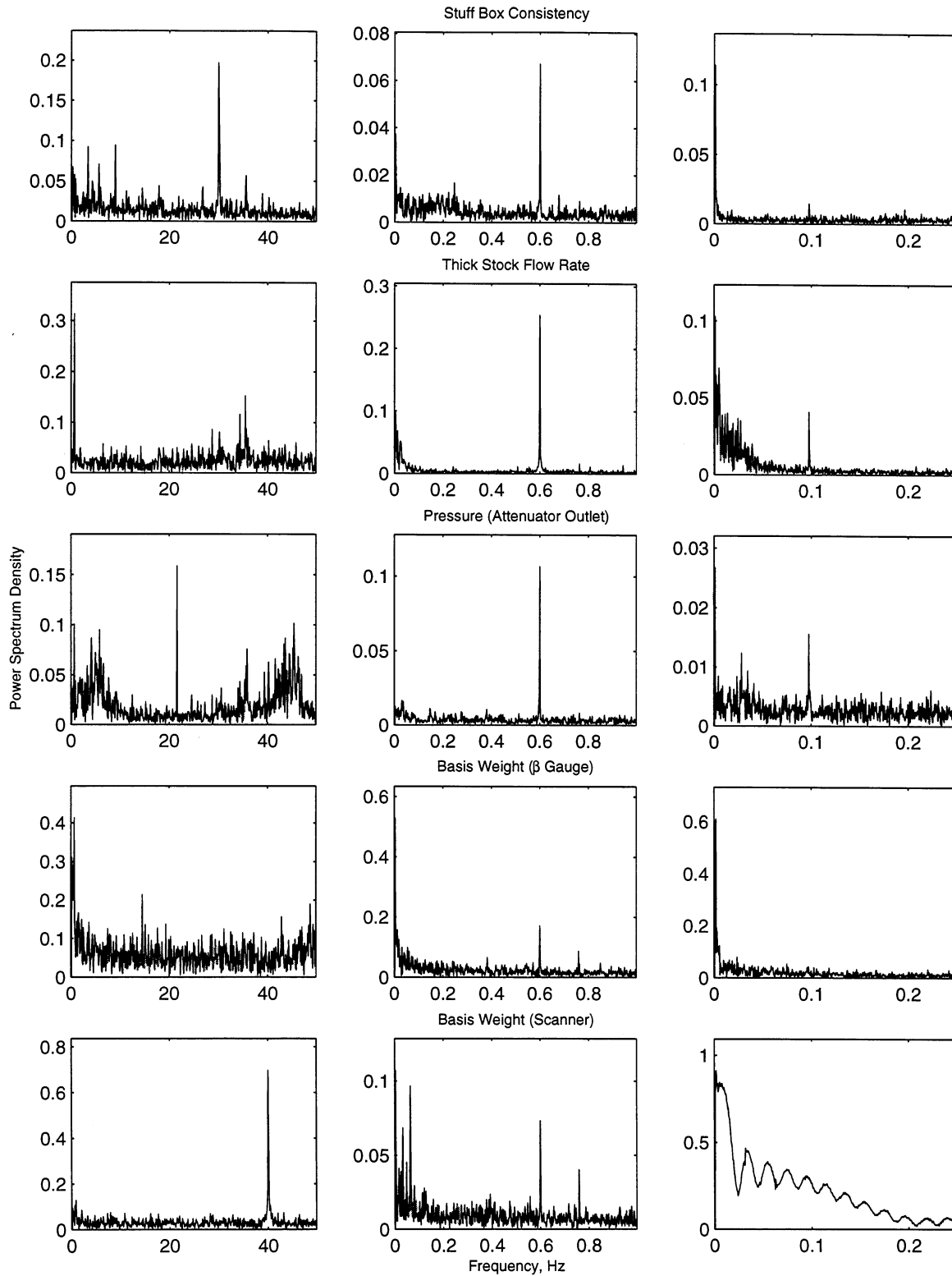Figure 4: Changes of process variables over time # 1. (Second run of 0.8917 hour)

17

Figure 5: Changes of process variables over time # 2. (Second run of 0.8917 hour)

18

Figure 6: Typical spectra of various signals within different frequency ranges. (First run of 2.817 hours)
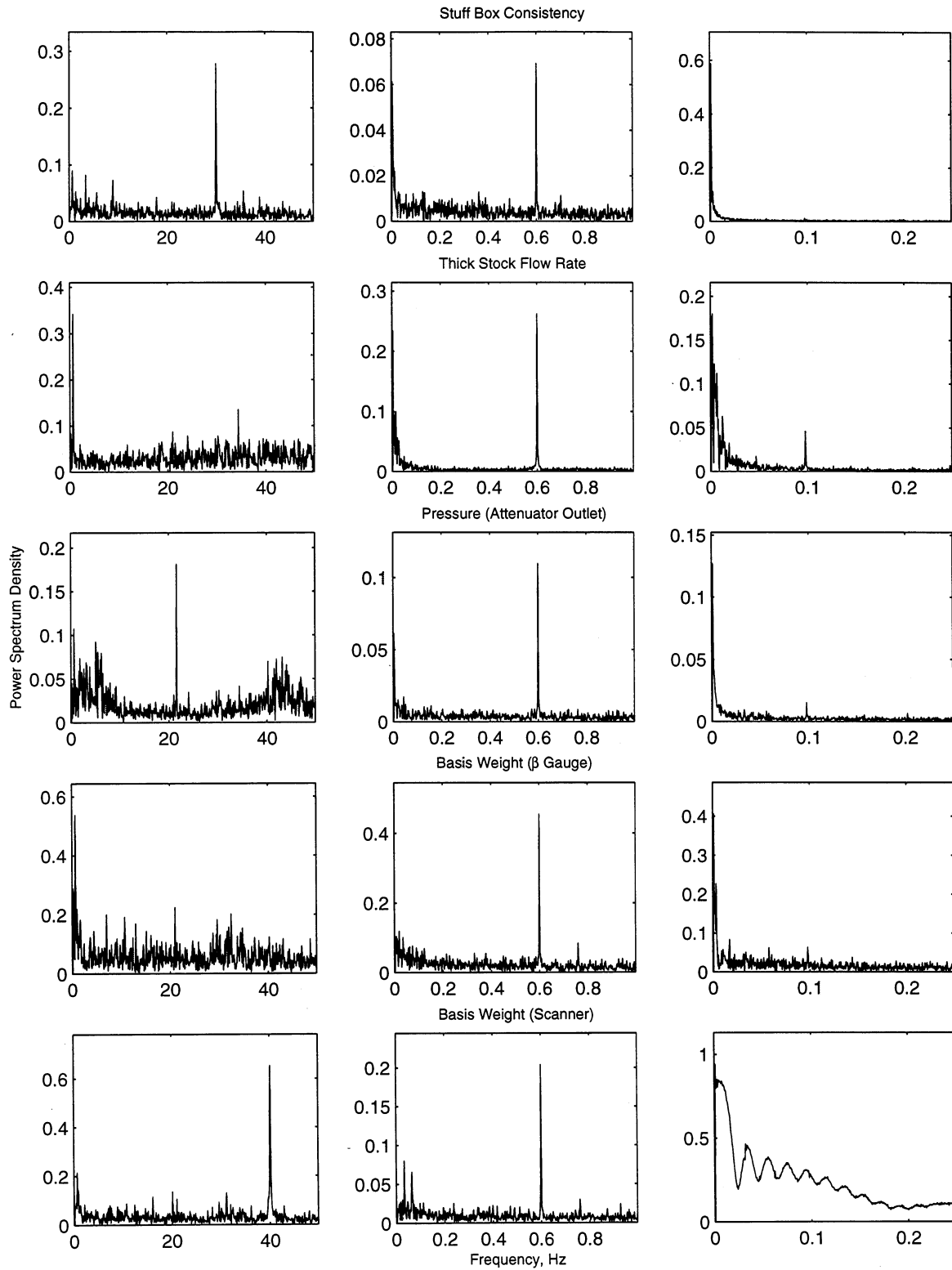
Figure 7: Typical spectra of various signals within different frequency ranges. (Second run of 0.8917 hour)
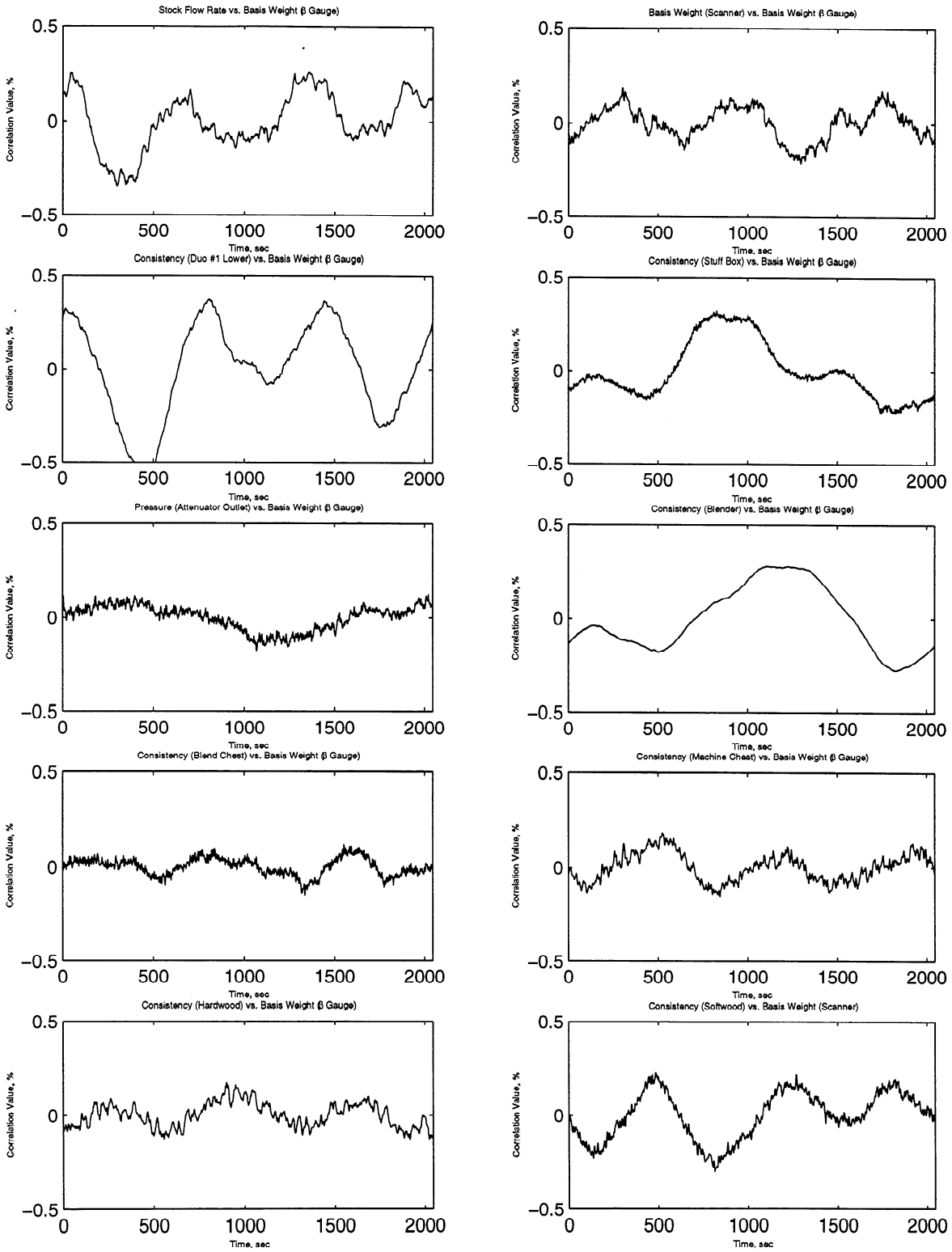
Figure 8: Cross correlations of low frequency variations. (First run of 2.817 hours)

21
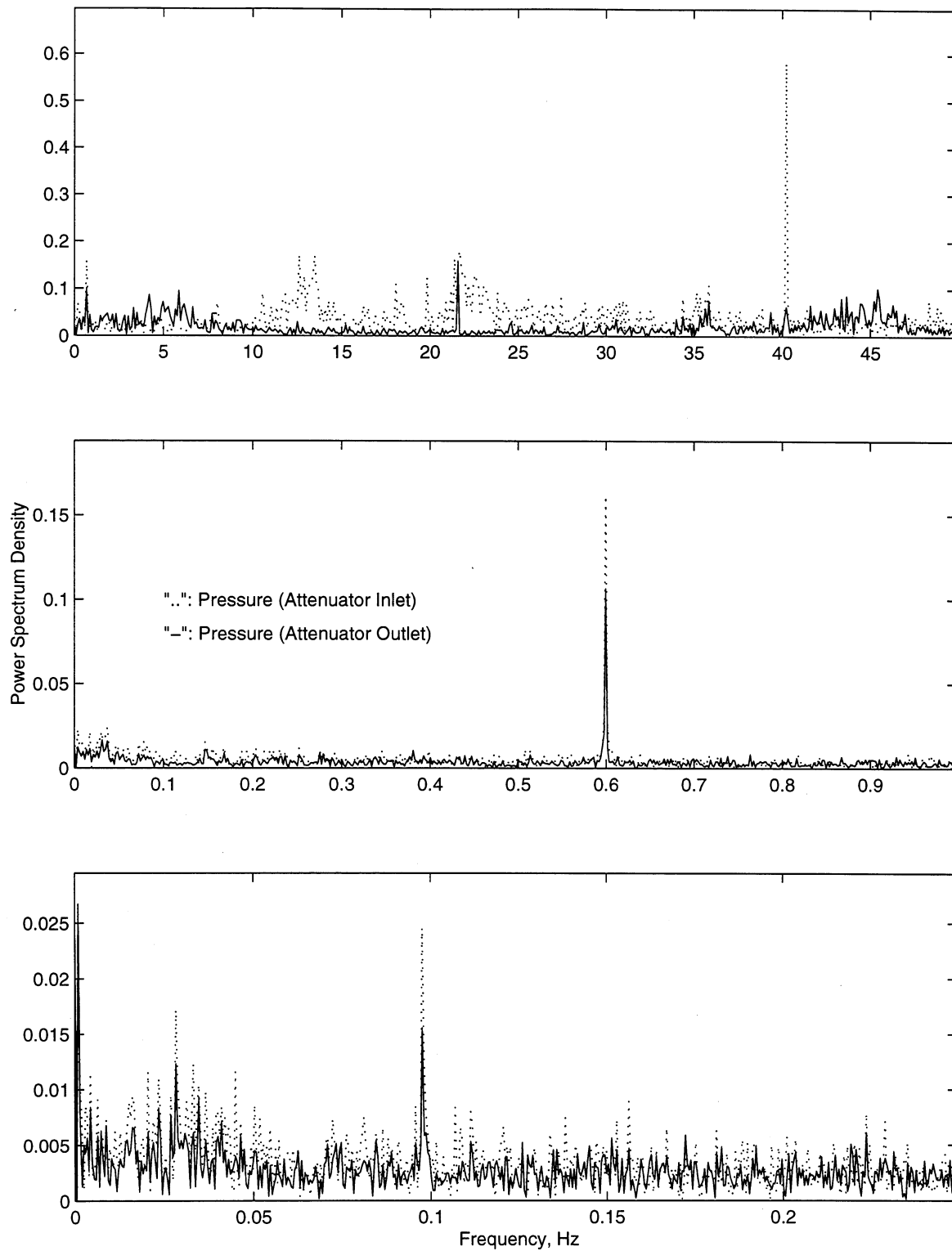
Figure 9: Effects of the pressure pulsation attenuator within three frequency ranges. (First run of 2.817 hours)
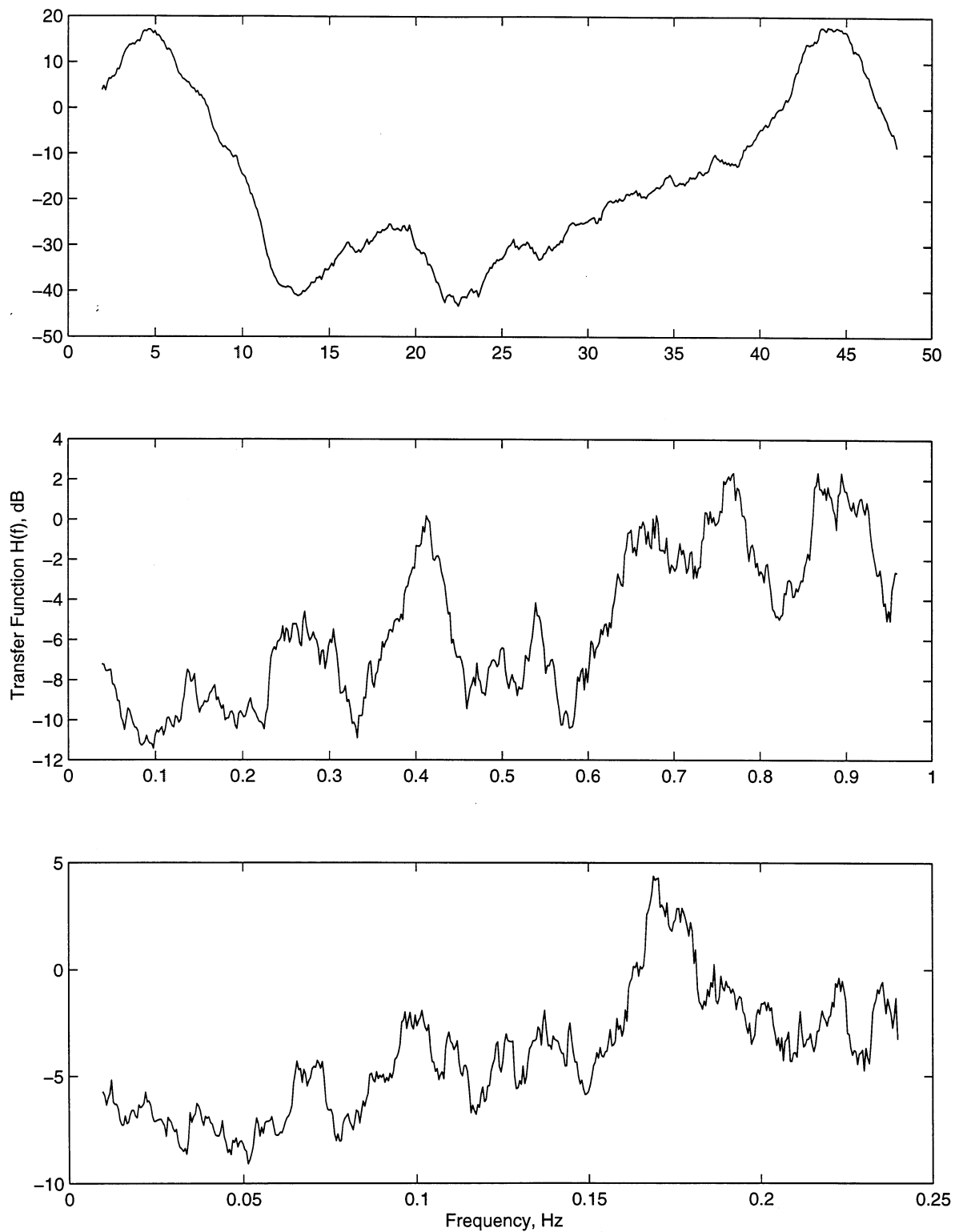
Figure 10: Transfer functions of the pressure pulsation attenuator. (First run of 2.817 hours)
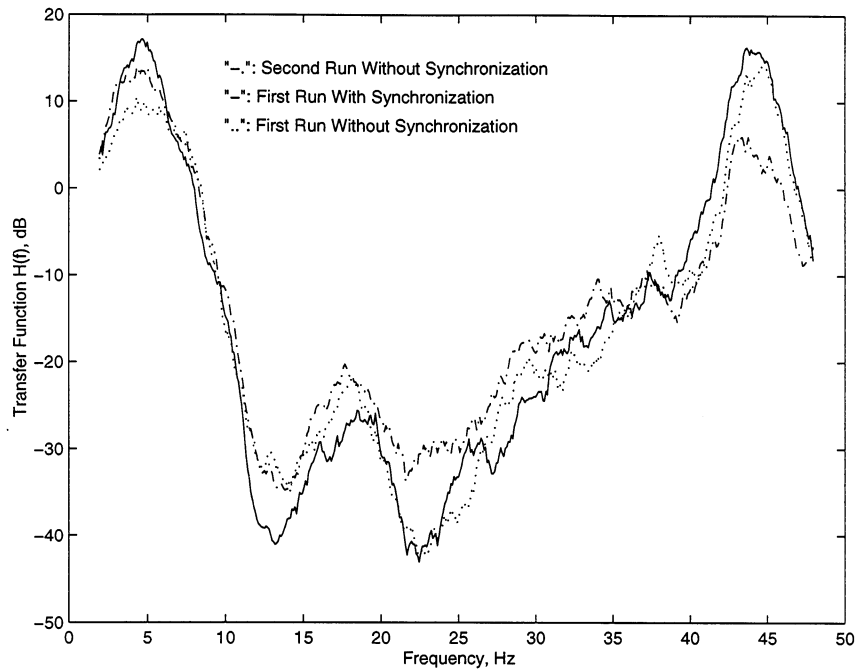
Figure 11: Time delay and synchronization effects on the transfer function of the pressure pulsation attenuator. (High frequency range with $N_a = 1$)
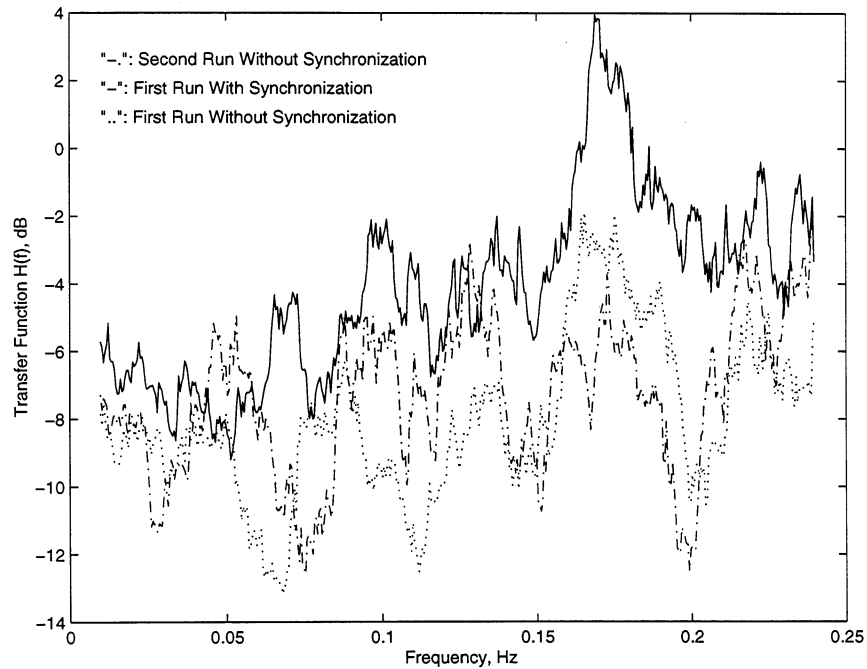
Figure 12: Time delay and synchronization effects on the transfer function of the pressure pulsation attenuator. (Low frequency range with $N_a = 200$)

24
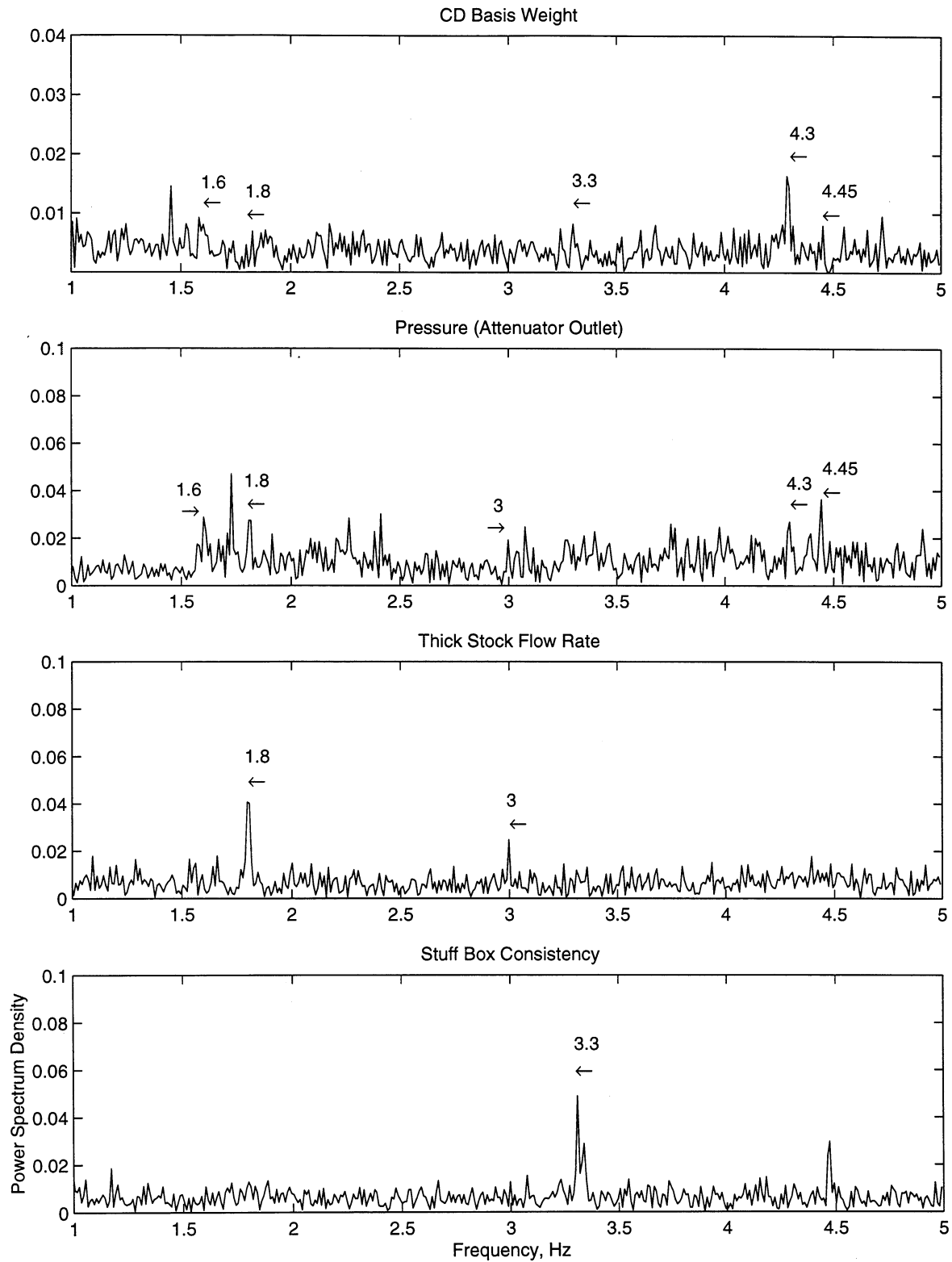
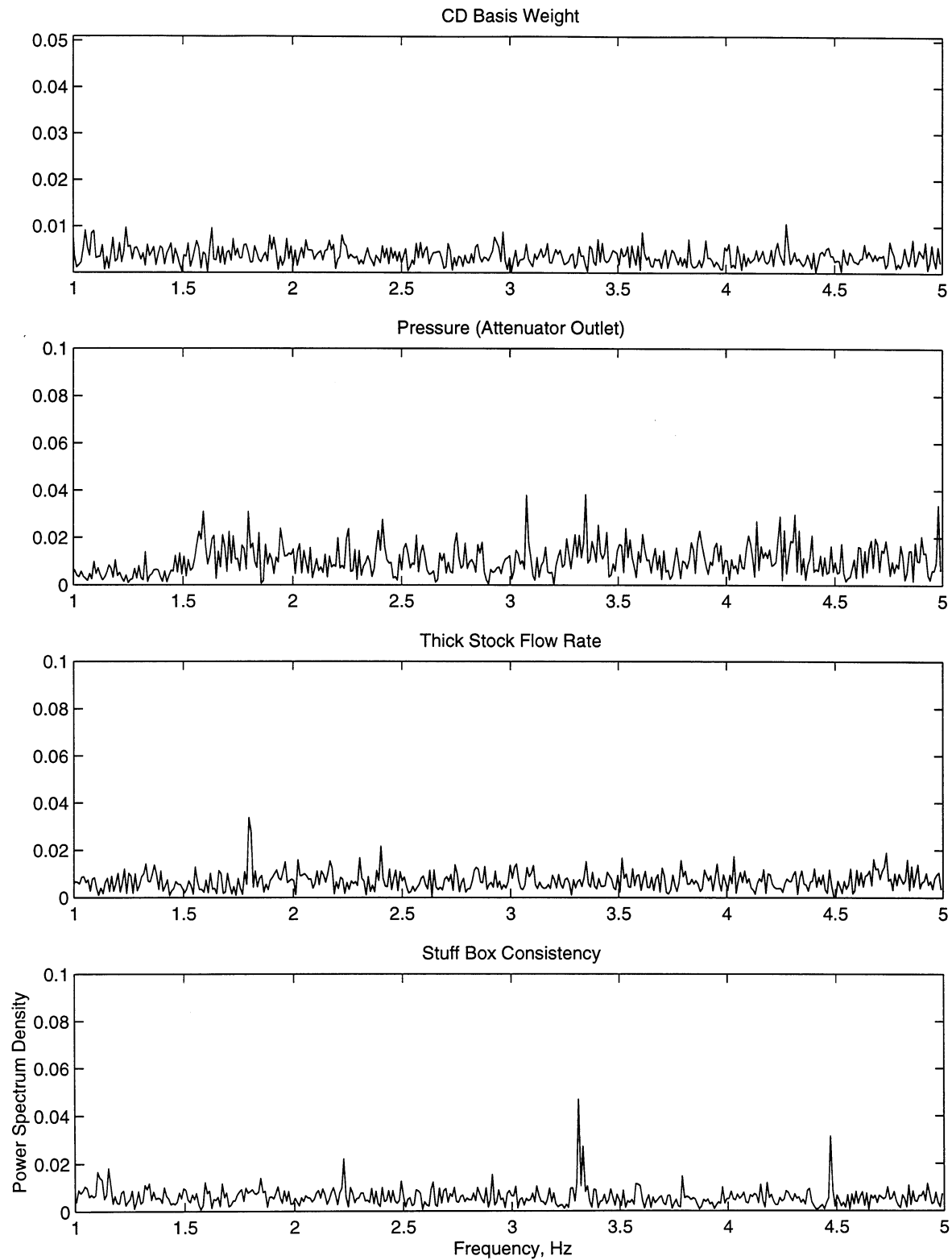Figure 13: Typical spectra associated with basis weight variations. (First run of 2.817 hours)

Figure 14: Typical spectra associated with basis weight variations. (Second run of 0.8917 hour)
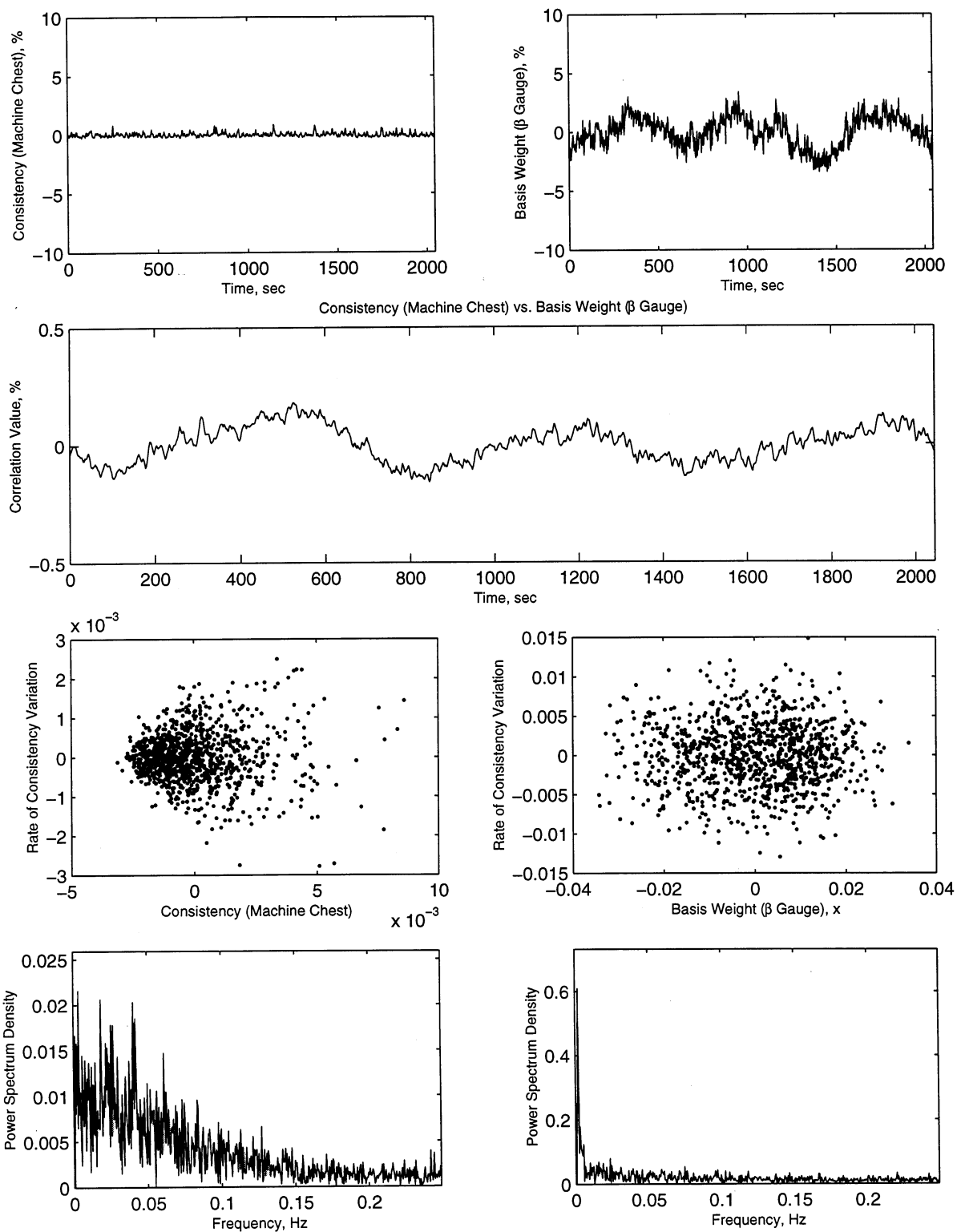
Figure 15: Correlation, phase-space, and spectrum plots of low frequency range signals of consistency and basis weight. (First run of 2.817 hours)
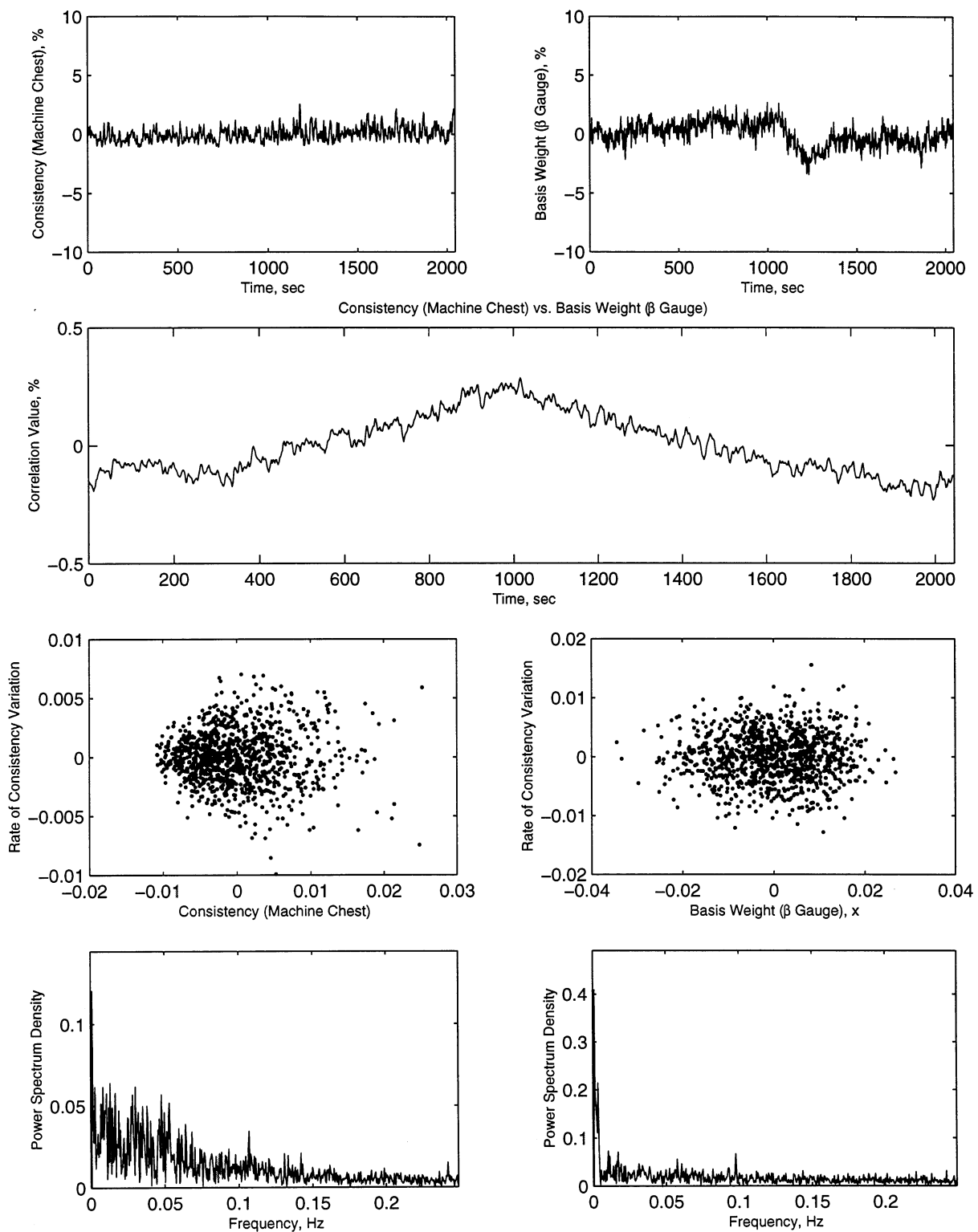
Figure 16: Correlation, phase-space, and spectrum plots of low frequency range signals of consistency and basis weight. (Second run of 0.8917 hour)
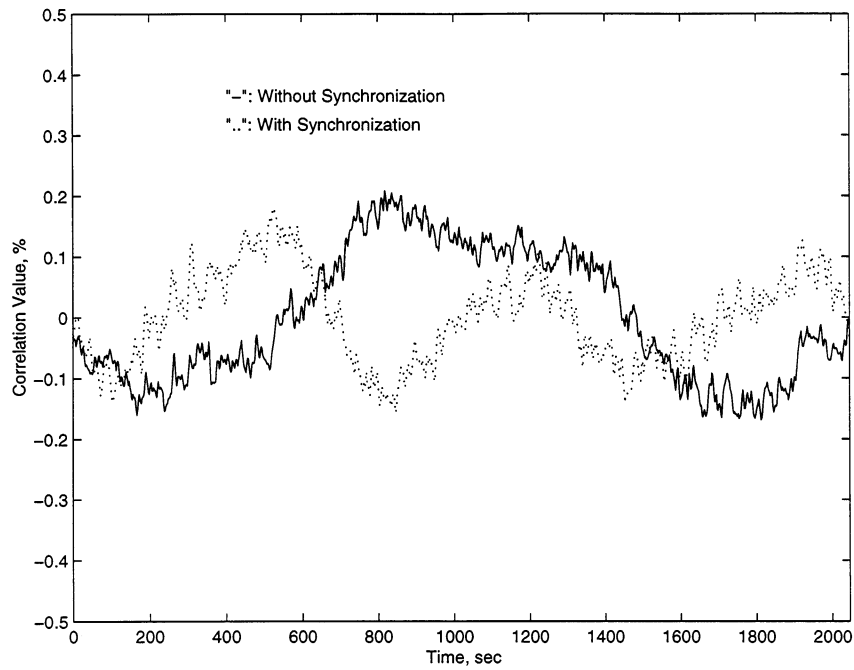
Figure 17: Synchronization effects on the cross correlation results. (First run of 2.817 hours)
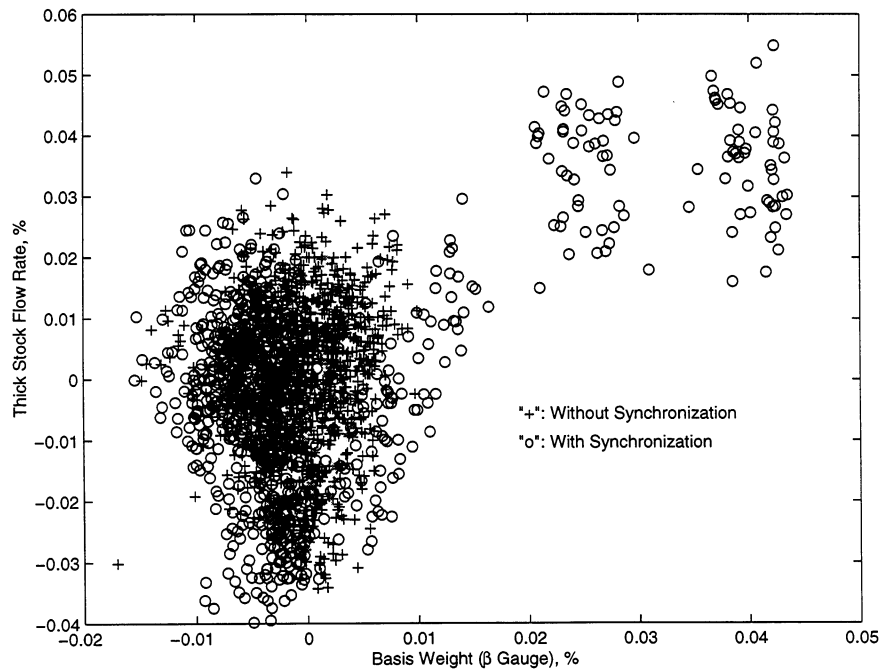

Figure 18: Scatter diagram of the thick stock flow rate *vs.* the β gauge measurement. (First run measurement, $N_a = 200$)
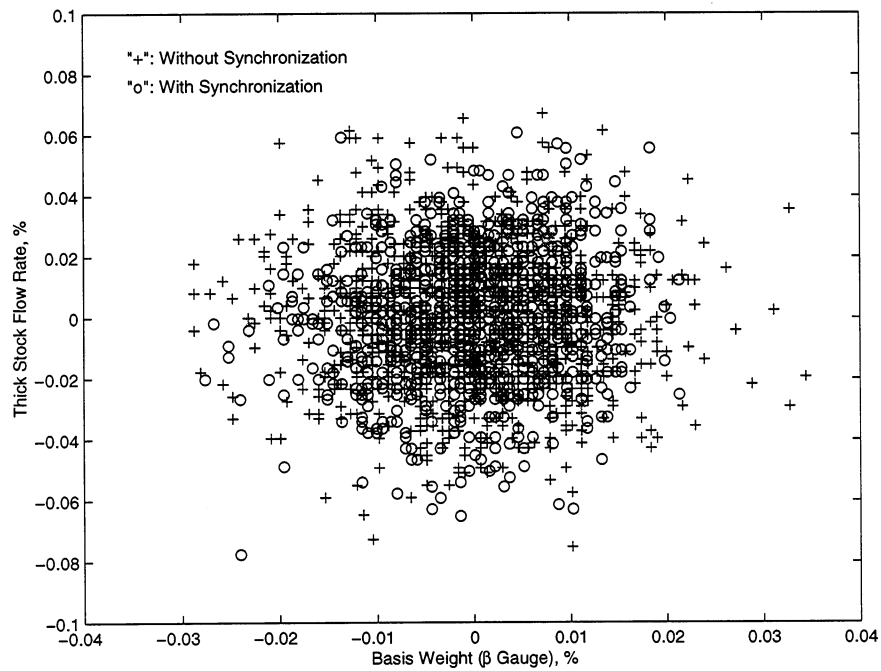
29

Figure 19: Scatter diagram of the thick stock flow rate *vs.* the β gauge measurement. (First run measurement, $N_a = 1$)

References

[1] R.C. Brendemuehl and J.E. Borchert. Real-time spectral analysis of machine directional basis weight variations in paper. *Tappi Journal*, 59(8):79–81, 1976.

[2] G. Burkhard and P.E. Wrist. The evaluation of paper-machine stock systems by basis-weight analysis. *Pulp and Paper Magazine of Canada*, pages 188–200, December 1954.

[3] J.W. Burns. The use of analysis of variance to characterize paper web non-uniformities. *Tappi Journal*, 57(12):143–146, 1974.

[4] Jere W. Crouse. Stock system pulsations - A cause of machine directional basis weight variations in paper. *Tappi Journal*, 59(8):76–78, 1976.

[5] W.H. Cuffey and G. Ingram. Cyclic machine direction basis weight variations. *Pulp and Paper Magazine of Canada*, pages T203–T215, April 1962.

[6] K.A. Cutshall. The nature of paper variation. *Tappi Journal*, pages 81–90, June 1990.

[7] K.A. Cutshall, G.E. Ilott, and J.H. Rogers. Grammage variation -Measurement and analysis. *TechSect CPPA Monograph*, 1988.

[8] K.A. Cutshall and J. Mardon. Causes of instability in paper machine wet ends. *Appita*, 28(4):252–260, 1975.

[9] J.M. Gess and R.A. Kanitz. Monitoring the stability of a paper machine. *Tappi Journal*, 79(4):119–126, 1996.

[10] B. Norman and D. Wahren. A comprehensive method for the description of mass distribution in sheets and flocculation and turbulence in suspensions. *Svensk Papperstidning årg*, 75(20):807–818, 1972.

[11] J.R. Parker and J.B.A. Epton. Practical investigation of grammage variations. *Pulp & Paper Canada*, 78(11):T245–T248, 1977.

[12] J. Perrault. The influence of wet-end vibrations on machine-direction basis-weight variations. *Tappi Short Course Notes – Wet End Operations*, pages 427–430, 1990.

[13] A. Rocheleau. A practical approach to the reduction of machine direction and cross direction basis weight variations. *Tappi Journal*, 48(9):48A–57A, 1965.

[14] A.G. Schöning and N. Jörgensen. Evaluation of wet end performance by basis-weight analysis. *Svensk Papperstidning årg*, 71(17):577–580, 1968.

[15] W.McC. Siebert. *Circuits, Signals, and Systems*. The MIT Press and McGraw-Hill Book Company, fourth edition, 1989.

[16] X. Wang and Z. Feng. A note on helmholtz attenuators with air cavity and membrane. *ASME Winter Meeting Symposium Program Noise and Vibration Control*, NVC-12, 1998.

[17] X. Wang, Z. Feng, and L.J. Forney. Computational simulation of turbulent mixing with mass transfer. *Computers & Structures*, 1998. In press.